Dynamic Characteristics of PWR Fuel Assemblies

A. Preumont, T. van Steenberghe
Belgonucléaire s.a.,
25 rue du Champ de Mars, B-1050 Bruxelles, Belgium

The state of the art analysis of a PWR core behaviour to dynamic events such as horizontal earthquake involves the time integration of the colliding vibration of a row of fuel assemblies. Such an analysis requires both a dynamic model of the fuel assemblies and an impact model of the spacer grids.

The first part of the paper is devoted to a fuel assembly dynamic model. It consists of two beams, representing respectively the skeleton and the fuel rods, connected together with rotary springs at the spacer grid levels :

- Skeleton : Experimental evidence shows that the shear deformations play a key-role in this beam ; its properties can be deduced from deflexion tests on the whole assembly.

- Fuel rods : The properties of this beam result directly from the fuel rod itself ; they are burn-up dependent, due to the clad creep-down, fuel swelling and plenum spring relaxation.

- Spacer grids : The rotary spring stiffness representing the rod to grid connection is deduced from static tests. It is dependant on the grid spring force and also, strongly, on the distance between the dimples, inside the spacer grid. For a particular design, such as BELGONUCLEAIRE's, involving two kinds of dimples, two beams may be necessary to represent the fuel rods.

Besides its simplicity allowing a direct introduction in the core model, this model gives a good representation of the low frequency vibrational behaviour of the fuel assembly. This is confirmed by comparison with experiments.

For the collinding vibration analysis of the core, the assumption is generally made that the shocks are restricted to the spacer grids, which are the widest components of the fuel assembly.

In the second part, static and impact tests carried out on Zircaloy spacer grids are briefly described. Experimental results are used to determine the stiffness and dissipation characteristics of a grid impact model consisting of a spring, viscous and hysteretic dampers. Soundness criteria are also discussed for OBE and SSE.

The final part of the paper describes briefly the core model and shows how the previous models are incorporated. The resulting computer program is named CLASH (Computer Program for Load on Assemblies under Seismic Horizontal Excitation). Its main feature is to use a two time-steps integration algorithm : the first one, related to the seismic excitation, applies to the assemblies not involved in shocks ; the second one, submultiple of the first one and related to the impact characteristics, is used for the others. It is then applied to a particular PWR core for which typical output (spacer grids displacements, inter-assemblies contact forces) are displayed.

1. INTRODUCTION

The PWR's core seismic analysis [1] requires a dynamic model of the fuel assembly. A simple model is presented. Further studies are still needed in view of the design applications, namely (i) the combined analysis of earthquake and LOCA ; (ii) the dynamic behaviour of the spacer grids, particularly beyond the elastic range ; (iii) the irradiation effect on the spacer grid dynamic properties, mainly the embrittlement.

2. VIBRATIONAL MODEL OF A PWR - RCC FUEL ASSEMBLY

2.1. Influence of Shear Deformations

Figure 1 shows the equivalent bending stiffness (bending stiffness of a single beam having the same displacements at one of spacer grids, for the same loading and support conditions) of a 14 x 14 (6 spacer grids) fuel assembly, for two different boundary conditions : (i) simply supported at the top, clamped at the bottom, loaded at the 4th spacer grid ; (ii) clamped at the bottom and loaded at the top. Decreasing bending stiffness as the load increases indicates a non-linear (softening) behaviour of the assembly. For a given load, different results are obtained for the various spacer grids ; this scattering indicates deviations between the fuel assembly and the beam model. The equivalent bending stiffness varies considerably with the support conditions ; this indicates a very poor representation of this kind of beam model.

However, including shear deformations (which are much more important, with respect to the bending deformations, for the first boundary conditions) improves considerably the agreement of a beam model, provided a large value is adopted for the parameter

$$\alpha = \frac{EI}{G\Omega' l^2} = \frac{EI}{Gk'}\left(\frac{r}{l}\right)^2 \cong 0.12 \text{ to } 0.15 \qquad (1)$$

where E stands for the Young's modulus, G is the shear modulus, $\Omega' = k'A$ is the effective shear area of the section, l is the length of the beam and $r = \sqrt{I/A}$ is the radius of gyration of the cross section.

The two-beam model described below includes shear deformations ; it can be seen in Figure 2 that it gives results in good agreement with the experiment, for both boundary conditions.

The boundary conditions of a fuel assembly in a nuclear reactor core can conveniently be represented by an embedment at the bottom, and a rotary spring at the top. Actually, the displacements in the central part of the assembly are rather insensitive to the rotary spring stiffness K_α, since their largest part result from shear deformations.

2.2. Vibrational Model of the Assembly

The vibrational model of the fuel assembly must account for :

(1) the static stiffness properties of the fuel assembly, as discussed in the previous sections ;

(2) the individual vibrational behaviour of the fuel rods, which constitute most of the assembly mass.

A previous analysis has shown that the low amplitude vibrations of the fuel rods can adequately be represented by a beam model (without shear deformations) with the following properties :

- the mass per unit length results from both the fuel pellets and the cladding tube ;
- the fuel pellets do not contribute to the rigidity of the rod ;
- the clad to spacer grid connection is modellized by a rotary spring. Its stiffness K_θ can

be determined by a simple static test ; it depends on the grid spring force and also, strongly, on the distance between the dimples inside the grid cells.

These considerations lead to the two-beam model of Figure 2.a, representing respectively the skeleton and the fuel rods. The first one includes the shear deformations, as stated earlier, and is mainly responsible for the static behaviour of the assembly. The second one simply adds the stiffness and mass properties of the fuel rods. They are connected by rotary springs at the grid levels, of which stiffness is simply the sum of individual stiffness of the rod-to-grid connection. If several groups of fuel rods, e.g. corresponding to different values of the distance between the dimples inside the grid cells are present in the assembly, as it is the case in BELGONUCLEAIRE's Zircaloy grids, then either a mean value is adopted for K_θ and a two-beam model is used (with the consequence of introducing one single natural frequency for all the fuel rods) or a three-beam model is adopted, with two values $K_{\theta 1}$ and $K_{\theta 2}$ for the clad to grid connection stiffnesses. Such a model is shown in Figure 3 for the 14 x 14 fuel assembly. It consists of a 55 degree of freedom (d.o.f.) Finite Element (F.E.) model ; modes 1 to 6 are also displayed. The first modes are representative of a single beam, they progressively deviate, as the order increases. Modes 5 and 6 are local fuel rods modes ; their frequencies depend mainly of the stiffness K_θ, as can be seen in table 1 for the two-beam model. A parametric study (table 1) has shown that the stiffness K_α does not influence strongly the results, as already mentionned.

Table 2 gives experimental natural frequencies of PWR fuel assemblies [2,3,4,5] ; their comparison with the column No. 2 of table 1 is excellent, as can be seen in Figure 4, except for the mode 5 for which the comparison is meaningless since this mode is a local mode for the fuel rods, in table 1. The agreement is particularly good with ref. [5] results which are relevant to the same kind of fuel assembly (14 x 14, 6 spacer grids).

The ultimate use of such a model being a non-linear core analysis, it is important to limit its number of d.o.f. The Guyan's reduction [6] can contribute significantly in this way. It expresses the eigen-value problem in terms of some selected (independent) d.o.f. by assuming a static relationship for the other (dependent) d.o.f. Such a condensation leads to a good estimate of the modes with natural frequencies f_i satisfying :

$$\frac{f_i}{\nu_1} \ll 1 \qquad (2)$$

where ν_1 is the first natural frequency of the system when all the independent d.o.f. have been clamped. The computation of ν_1 can help considerably in the choice of the independent d.o.f. This is illustrated in table 3 where 3 different reductions are compared ; the nodes numbering refers to Figure 3. The comparison of cases 2 and 3 shows that an adequate choice of the d.o.f. can increase considerably the adequacy of the reduction : a slightly different choice of the 30 independent d.o.f. rise the frequency ν_1 from 174.4 to 324.5 Hz.

3. SPACER GRIDS IMPACT BEHAVIOUR

3.1. Spacer Grid Dynamic Model

In the core model, the spacer grids are modellized by impact elements consisting of springs, viscous and hysteretic dampers (Figure 5.a). This impact element includes the two-elements of figure 5.b and c :

a. Spring and Hysteretic Damper (Figure 5.c) : this element has been used by Nuno et al. [7].

Its constitutive equation is :

$$f = \begin{cases} (k + h)\, x & (\dot{x} > 0) \\ (k - h)\, x & (\dot{x} < 0) \end{cases} \qquad (3)$$

It has the remarkable property of having a restitution coefficient which depends only on the impact element itself, and not on the initial velocity v_o, nor on the impacting mass.

$$r = -\frac{v}{v_o} = \sqrt{\frac{k - h}{k + h}} \qquad (4)$$

b. Spring and Viscous Damper (Figure 5.b) : its constitutive equation is :

$$f = kx + c\dot{x} \qquad (5)$$

The coefficient of restitution is approximately given by :

$$r \cong e^{-\pi\xi} \ (\xi \ll 1), \text{ where } \xi = \frac{c}{2\sqrt{km}} \qquad (6)$$

It depends explicitely on the impacting mass m and will vary from one spacer grid to another. In a comparison [8] between these models, the viscous damping coefficient was chosen in order to have the same restitution coefficient (0.8) for the maximum mass translational d.o.f. of a spacer grid (d.o.f. 3, node 18, in table 3). Only slight differences in the grids displacements and impact forces were observed.

3.2. Test Results

Figure 6 shows the results of static compression tests performed on BELGONUCLEAIRE's 14 x 14 Zircaloy spacer grids. The shaded area is the total elastic energy E_e (1.6 Nm in Figure 6) that can possibly be stored in the grid, before instability. The following expression has been adopted for the maximum strain energy in the impact elements :

$$E_d = \frac{1}{2}\left(\frac{F_{max}^2}{k + h}\right)$$

where F_{max} is the maximum contact force between assemblies. The assembly will remain within the elastic range provided $E_d \leq E_e/2$ (since the spacer grid is represented by two impact elements). This criterion is more advantageous that any other based on the maximum impact force because (i) the results of the core model, in terms of E_d instead of F_{max}, are less sensitive to the spring stiffness k ; (ii) the spacer grids actual characteristics are non linear while their model is linear, leading to some problems in the choice of k.

Figure 7 shows preliminary impact test results obtained on 5 x 5 spacer grids (without any fuel rods). It can be seen that, beyond the elastic range (where those tests have been performed), the restitution coefficient depends on the impact velocity v_o, as well as on the number of impacts N. This is confirmed by Figure 8 where two velocity diagrams are displayed for impacts No. 2 and 13, on the same sample grid : it is clear that the restitution coefficient and the shock duration both increase (implying a decrease of the spring stiffness k) as the number of impacts increases.

3.3. Earthquake Design Criteria

According to the Standard Review Plan (section 4.2, fuel system design), the following design criteria must be fulfilled for both the SSE (Safe Shutdown Earthquake) and the OBE (Operating Basis Earthquake).

a. The fuel system damage is never so severe as to prevent the control rod insertion.

b. The fuel assembly retains its rod-bundle geometry with adequate coolant channels to permit removal of the residual heat.

In structural terms, this implies that the spacer grids neither suffer a brittle fracture, nor the plastic deformations exceed a definite value, necessary for the control rods insertion and the coolability.

Besides those criteria, 2 possibilities can be considered for the OBE, depending on economic consideration : (i) the core must remain undamaged in order to restart the reactor without unloading ; the assembly must then remain within the elastic range ; (ii) it is acceptable to waste the whole core and only the unloading capability must be assured.

4. EXAMPLE OF APPLICATION

The fuel assembly finite element model and the spacer grids dynamic model have been introduced in the computer program CLASH [1] which study the colliding vibration of a row of fuel assemblies under seismic excitation from the core plates. It has been applied to the Belgian DOEL reactor, the core plates accelerogram adopted is diplayed in Figure 5 of [1] ; it corresponds to a 0.1 g maximum ground acceleration. This accelerogram has also been doubled, in order to simulate a 0.2 g maximum ground acceleration. The results are summarized in table 4, the core response is illustrated in Figure 9. One can see that the limit of $E_e/2$ = 0.8 Nm is not exceeded in the 0.1 g case. The E_d value obtained in the 0.2 g case is well above the elastic limit ; plastic deformations are therefore expected in this case ; they could be evaluated with curves similar to those of Figure 7.b. More details are given in [8].

5. REFERENCES

[1] A. PREUMONT, "A Two Time Step Algorithm for Seismic Analysis of a PWR Core", Submitted for publication in Nuclear Engineering and Design.

[2] Y. TIGEOT, P. BULAND, "Analyse du comportement vibratoire des assemblages combustibles destinés à équiper les réacteurs de puissance du type "eau ordinaire sous pression"", BIST, CEA n° 213, avril 1976.

[3] F.E. STOKES, R.A. KING, "PWR Fuel Assembly Dynamic Characteristics", BNES, Vibration in Nuclear Plant, Keswick - UK, May 1978.

[4] H. NUNO et al., SMIRT-4, San Francisco 1977, paper D 4/6.

[5] Aimablement communiqué par la société FRAMATOME (siège de Lyon).

[6] R.J. GUYAN, "Reduction of Stiffness and Mass Matrix", AIAA Journal, Vol 3, No. 2, 1965.

[7] H. NUNO et al., SMIRT-2, Berlin 1973, paper K 6/10.

[8] A. PREUMONT, "Analyse sismique du coeur d'un réacteur PWR", Thèse de doctorat, Université de Liège, 1981.

- TABLE 1 -

14 x 14, 6 SPACER GRIDS FUEL ASSEMBLY. TWO-BEAM FINITE ELEMENT MODEL PARAMETRIC STUDY ON K_α AND K_θ VALUES

	$K_\alpha = 10^4$ Nm/rad $K_\theta = 179 \times 300$ Nm/rad		$K_\alpha = 10^5$ Nm/rad $K_\theta = 179 \times 300$ Nm/rad		$K_\alpha = 10^5$ Nm/rad $K_\theta = 179 \times 200$ Nm/rad	
Mode i	f_i(Hz)	f_i / f_1	f_i(Hz)	f_i/f_1*	f_i(Hz)	f_i / f_1
1	6,33	1	6,50	1	6,25	1
2	14,62	2,31	14,71	2,26	14,10	2,26
3	23,72	3,75	23,84	3,67	22,90	3,66
4	34,34	5,42	34,48	5,30	33,36	5,34
5	50,23	7,94	50,58	7,78	47,21	7,55
6	62,62	9,89	63,20	9,72	61,08	9,77

* THOSE VALUES ARE DISPLAYED ON FIGURE 4.

- TABLE 2 -

NATURAL FREQUENCIES OF PWR - RCC FUEL ASSEMBLIES
EXPERIMENTAL DATA (Hz)

	CEA 15 x 15 7 SP. GR. [2]		B & W 17 x 17 8 SP. GR. [3]	MITSUBISHI 14 x 14 [4]	FRAMATOME 14 x 14 6 SP. GR. [5]	
MODE	f_i	f_i/f_1	f_i/f_1	f_i/f_1 *	f_i	f_i/f_1
1	3.7	1	1	1	6.50	1
2	7.63	2.05	1.9	2.3	13.21	2.03
3	11.67	3.15	3	3.6	22.05	3.39
4	18.55	5.01	4.1	5.1	30.55	4.7
5	24.78	6.7	5.3	6.6	**	
6	38.31	9.87			62.16	9.56
7					78.93	12.14

* APPROXIMATE VALUES ESTIMATED FROM GRAPHS.
** A FUEL ROD LOCAL MODE IS MISSING HERE.

- TABLE 3 -

COMPARISON OF VARIOUS CASES OF GUYAN'S REDUCTIONS

NODES (FIG.3)	INDEPENDENT DEGREE OF FREEDOM								
	F.E. MODEL		GUYAN'S REDUCTION						
			CASE 1		CASE 2		CASE 3		
2	3	5							
3		5							
5		5							
7	3	5			3		3		
8	3	5	3		3	5	3	5	
9	3	5	3		3	5	3	5	
10	3	5	3	5	3	5	3		
11		5							
13		5							
15	3	5					3		
16	3	5	3		3	5	3	5	
17	3	5	3		3	5	3	5	
18	3	5	3	5	3	5	3		
19		5							
21		5							
23	3	5					3		
24	3	5	3		3	5	3	5	
25	3	5	3		3	5	3	5	
26	3	5	3	5	3	5	3		
27		5							
29		5							
31	3	5					3		
32	3	5	3		3	5	3	5	
33	3	5	3		3	5	3	5	
34	3	5	3	5	3	5	3		
35		5							
37		5							
39	3	5			3		3		
40	3	5	3		3	5	3	5	
41	3	5	3		3	5	3	5	
42	3	5					3		
43		5							
45		5							
47		5							
NUMBER OF D.O.F.	55		18		30		30		
FIRST NATURAL FREQUENCY ν_1 INDEPENDENT D.O.F. CLAMPED			144,4 Hz		174,4 Hz		324,5 Hz		

- TABLE 4 -

ROW OF 10 FUEL ASSEMBLIES, 10 S DURATION
CLASH RESULTS

MAXIMUM GROUND ACCELERATION	MOST SEVERE IMPACT			CPU* (S)
	F_{MAX} (N)	E_d (Nm)	AT t = (SEC)	
0.1 g	3483	0.253	4.477	1350
0.2 g	10140	2.14	3.125	2945

* CYBER 174 SCOPE 3.4

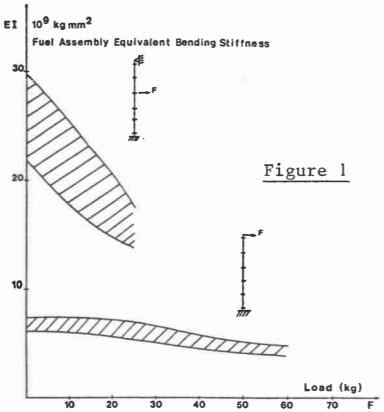

Figure 1

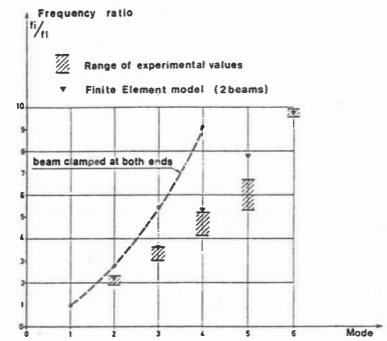

Figure 4

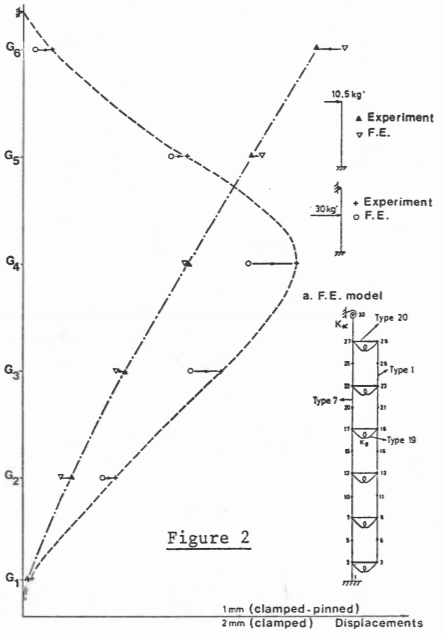

Figure 2

b. Comparison between Finite Element model and Experiment

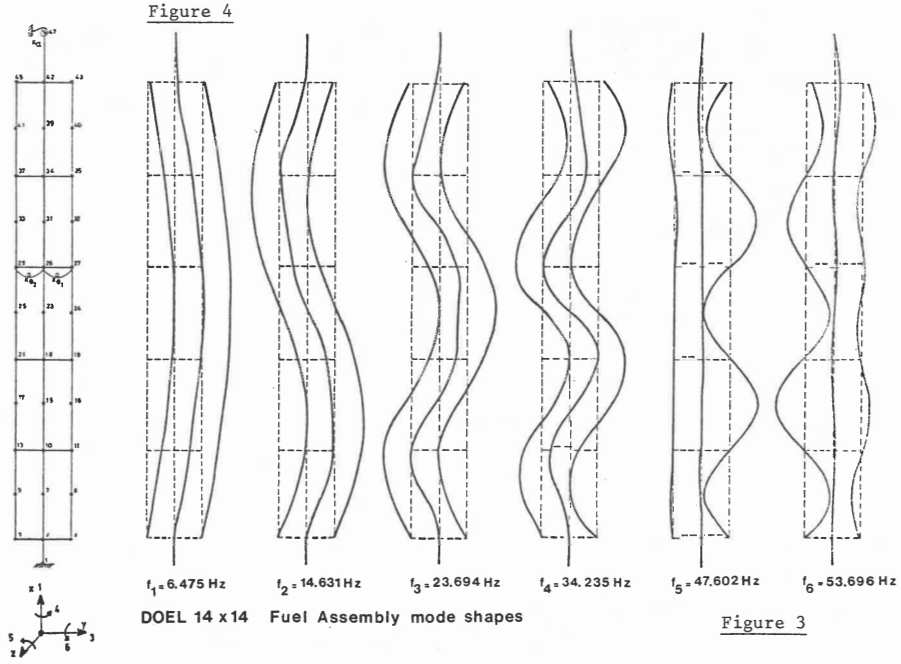

DOEL 14 x 14 Fuel Assembly mode shapes

Figure 3

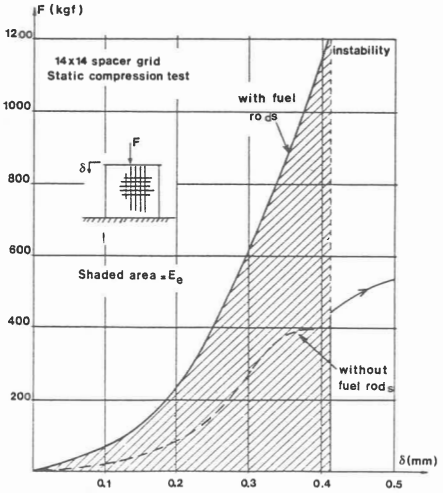

Figure 6 : Static Compression Test Results

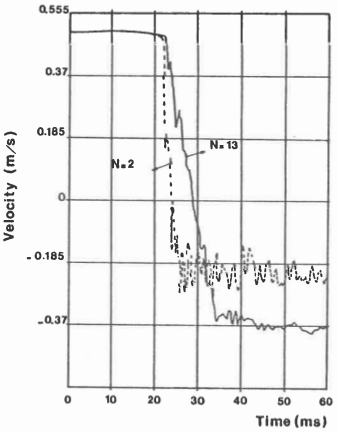

Figure 8 : Velocity Diagram during Impact

Figure 5 :

Ⓐ Spacer grid representation in the core model

Ⓑ Spring and viscous damper impact element

$$f = kx + c\dot{x}$$

$$r \cong e^{-\pi\xi} \qquad \xi = \frac{c}{2\sqrt{km}}$$

$$(\xi \ll 1)$$

Ⓒ Spring and hysteretic damper impact element

$$f = \begin{cases} (k+h)x & (\dot{x} > 0) \\ (k-h)x & (\dot{x} < 0) \end{cases}$$

$$r = -V/V_o = \sqrt{k-h/k+h}$$

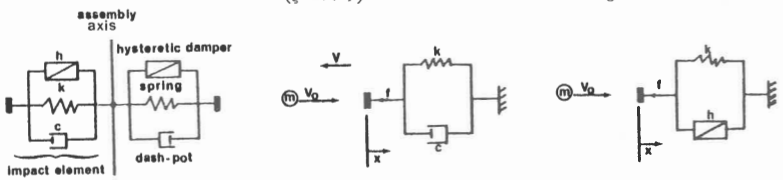

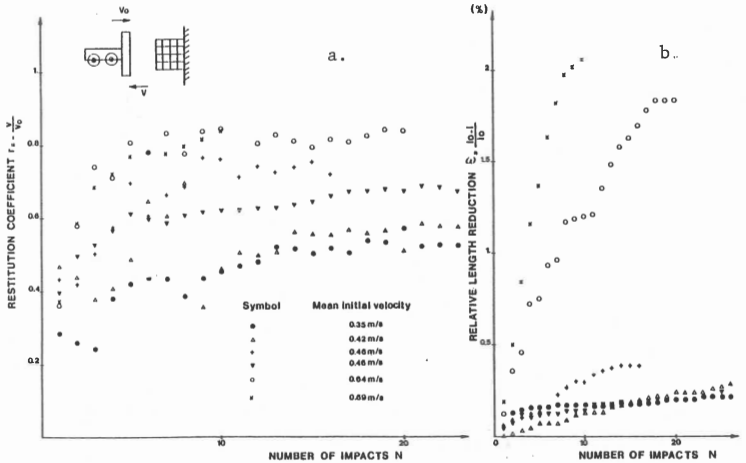

Figure 7 : Impact Test Results on 5 x 5 Dummy Zircaloy Spacer Grids

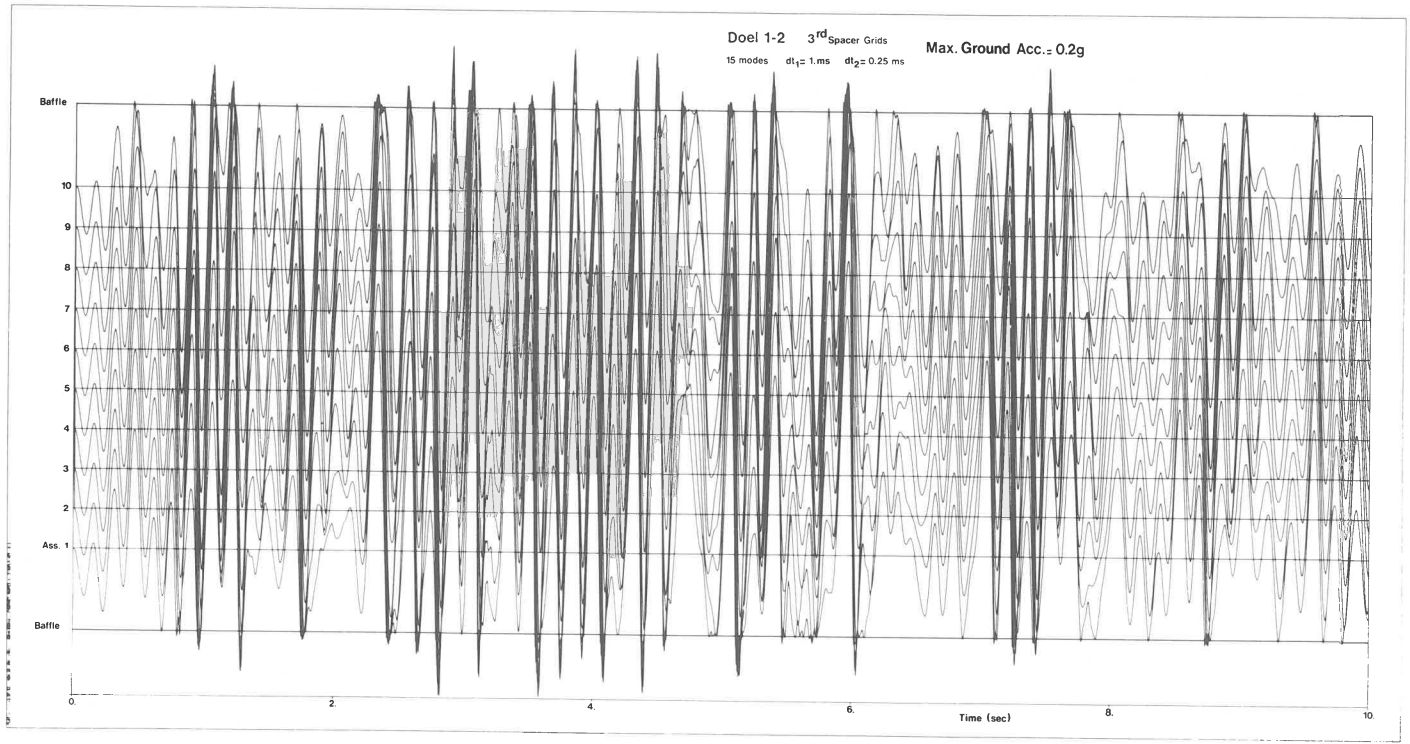

Figure 9 : 14 x 14 - 6 spacer grids fuel assembly
Row of 10 assemblies
3rd level spacer grids displacements